www.rericjournal.ait.ac.th

Analysis of Thermohydraulic Performance of Double Flow V-Corrugated Absorber Solar Air Heater

Som Nath Saha*[1] and Suresh Prasad Sharma*

Abstract – In this paper the mathematical model of double flow flat plate and different angle of v-corrugated absorbers solar air heater are presented. A computer programme in C++ language is developed to estimate the temperature rise of entering air for evaluation of thermal and thermohydraulic efficiency also called "effective efficiency" by solving the governing equations numerically using relevant correlations for heat transfer coefficient for double flow v-corrugated absorber. The results obtained from the mathematical model is compared with available experimental results and found to compare well. The deviation in efficiency for flat plate and 60˚ v-corrugated absorber collectors is found to be in the range of ±5.47 % and 4.46 % respectively. The effect of fraction of mass flow rate (φ) on thermal efficiency and v-corrugated angle (θ) of absorber plate of double flow solar air heater have been analyze and found that at φ = 0.5 i.e. equal mass flow rate through both channels gives best performance. Also the comparison of the results of double flow flat plate with v-corrugated absorber of different angle show a substantial enhancement in efficiency with double flow v-configuration absorber. The 60˚ v-angle absorber maintains the highest efficiency values throughout the range of mass flow rates investigated. Again most efficient 60˚ v-corrugated absorber double flow solar air heater attains maximum value of thermohydraulic efficiency at air mass flow rate of 0.045 kg/s.

Keywords – fraction of mass flow rate, solar air heater, thermal efficiency, thermohydraulic efficiency, v-corrugated absorber.

1. INTRODUCTION

Demand of energy consumption is growing exponentially. Conventional sources of energy cannot fulfil the demand for long period of time. Alternative source of energy which can fulfil the demand is renewable sources of energy. Among all sources of renewable energy, solar energy is sustainable, abundant and clean. The application of solar energy is very wide i.e. heating, drying, cooking, power generation etc. The solar air heater is one of the important type of collector for the purpose of air heating. It is a specific type of heat exchanger which transfers heat energy, obtained by absorbing insolation. It can be used for many applications at low and moderate temperature. Some of these have been crop drying, timber seasoning, space heating etc. However, their usefulness as energy collection has been limited because of poor thermophysical properties of air, low convective heat transfer coefficient between the absorber plate and flowing air leads to higher plate temperature and greater thermal losses.

Several designs of solar air heaters have been developed over the years in order to improve their performance. Such design includes honeycomb collectors, extended surface absorber, use of artificial roughness on the absorber plate, packing of porous material in air flow channel. One of the effective ways to improve the convective heat transfer rate is to increase the heat transfer surface area and to increase turbulence inside the channel by using fin or corrugated surfaces [1], [2]. Ho-Ming *et al.* [3] investigated the performance of double flow solar air heater and found more effective than conventional solar air heater. Hikmet [4] presented energy and exergy analysis of a double flow flat plate solar air heater with several obstacles on absorber plate and without obstacles. The influence of fins and baffles attached over the absorber plate on the performance of single pass solar air heater investigated by Mohammadi and Sabzpooshani [5] and found that the outlet air temperature and efficiency are higher in comparison to conventional air heater. Pakdaman *et al.* [6] investigated experimentally to evaluate the performance of solar air heater with longitudinal rectangular fins array. Abhishek and Prabha [7] analyzed the performance of wavy finned absorber solar air heater. A comprehensive study of solar air heater having roughness elements on the absorber plate with different geometry was presented by Mittal *et al.* [8]. Paisarn [9] studied numerically about heat transfer characteristics and performance of double pass flat plate solar air heater with and without porous media. Vimal and Sharma [10] theoretically investigated the thermal performance of packed bed solar air heater with wire screen matrices. Taymaz *et al.* [11] experimentally investigated the convective heat transfer characteristics in a periodic converging diverging heat exchanger channel. The effects of the operating parameters on forced convection heat transfer for air flowing in a channel having v-corrugated upper plate and other walls are thermally insulated is studied by Ahmed *et al.* [12]. Fabbri [13] analysed the heat transfer in a channel having smooth and corrugated wall under laminar flow conditions and used finite element model to determine

*Department of Mechanical Engineering, National Institute of Technology, Jamshedpur, Jharkhand-831014, India.

[1]Corresponding author;
Tel: +91 8582094184.
Email: somnath.rvs@gmail.com

the velocity and temperature distributions. Nephon [14] investigated heat transfer characteristics and pressure drop in the channel with v-corrugated upper and lower plates. El-Sebaii *et al.* [15] investigated the performance of double pass flat and v-corrugated solar air heaters and found the double pass v-corrugated have 11-14 % more efficient than double pass flat plate heater. A parametric study of cross corrugated solar air collectors having wavelike absorbing plate and wavelike bottom plate crosswise position performed by Wenxian *et al.* [16] and Wenfeng *et al.* [17] and found that the cross corrugated collector have superior thermal performance than that of the flat plate. Yasin and Hakan [18] studied the natural convection heat transfer of inclined solar collectors and compared wavy absorber with flat absorber collectors. The flat plate and v-corrugated plate solar air heaters with phase change material as thermal energy storage investigated by Kabeel *et al.* [19] and they found that the v-corrugated plate solar air heater have better performance.

This paper present mathematical models to investigate analytically the thermal and thermo hydraulic (effective) performance of double flow flat (plane) and v-corrugated absorber solar air heaters with different v-angle (θ). The main features of the solar air heaters considered in this study; all type heaters consist of double glass cover, double flow and average air flow channel gap of 25 mm. The angles (θ) with different type of v-corrugated absorber solar air heater are assumed to be 30˚, 45˚, 60˚, 90˚ and 120˚.

2. THEORETICAL ANALYSIS

The mathematical models for flat and v-corrugated absorber solar air heaters are presented. The double flow flat plate solar air heater is presented in Figure 1. Two air streams are flowing simultaneously over (flow 1) and under (flow 2) the absorbing plate having different flow rates but total flow rate are constant. The formation of mathematical models is based on following assumptions: (i) air temperature variation is the function of the flow direction only. (ii) negligible temperature drop across the glass covers, absorbing and bottom plate. (iii) glass cover and flowing air do not absorb radiant energy. (iv) thermal losses through side and bottom insulation are negligible.

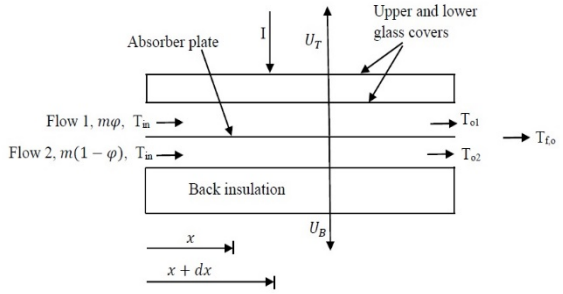

Fig. 1. The double flow flat plate solar air heater.

2.1 Energy Balance Equations

For the lower glass cover (cover 1),

$$h_{r,ap-gc1}(T_{ap} - T_{gc1}) + h_{c,f1-gc1}(T_{f1} - T_{gc1}) = U_{gc1-a}(T_{gc1} - T_a) \quad (1)$$

For the absorbing plate,

$$I\alpha_{ap}\tau_{gc}^2 = U_T(T_{ap} - T_a) + U_B(T_{ap} - T_a) + h_{c,ap-f1}(T_{ap} - T_{f1}) + h_{c,ap-f2}(T_{ap} - T_{f2}) \quad (2)$$

Rewriting the Equations 1 and 2, respectively

$$T_{f1} - T_{gc1} = \left(\frac{1}{h_{r,ap-gc1}+h_{c,f1-gc1}+U_{gc1-a}}\right)[-h_{r,ap-gc1}(T_{ap} - T_{f1}) + Ugc1{-}aTf1{-}Ta \quad (3)$$

$$T_{ap} - T_{f1} = -\left(\frac{U_T+U_B+h_{c,ap-f2}}{U_T+U_B+h_{c,ap-f1}+h_{c,ap-f2}}\right)(T_{f1} - T_a) + \left(\frac{h_{c,ap-f2}}{U_T+U_B+h_{c,ap-f1}+h_{c,ap-f2}}\right)(T_{f2} - T_a) + \left(\frac{I\alpha_{ap}\tau_{gc}^2}{U_T+U_B+h_{c,ap-f1}+h_{c,ap-f2}}\right) \quad (4)$$

$$T_{ap} - T_{f1} = -J_1(T_{f1} - T_a) + J_2(T_{f2} - T_a) + J_3 \quad (5)$$

Putting the expression $(T_{ap} - T_{f1})$ from Equation 5 into Equation 3, we have

$$T_{f1} - T_{gc1} = J_4[(U_{gc1-a} + J_1h_{r,ap-gc1})(T_{f1} - T_a) - J2hr,ap{-}gc1Tf2{-}Ta{-}hr,ap{-}gc1J3 \quad (6)$$

For the bottom plate,

$$h_{r,ap-bp}(T_{ap} - T_{bp}) + h_{c,f2-bp}(T_{f2} - T_{bp}) = U_{bp-a}(T_{bp} - T_a) \quad (7)$$

Rewriting the Equations 7 and 2, respectively

$$T_{f2} - T_{bp} = \left(\frac{1}{h_{r,ap-bp}+h_{c,f2-bp}+U_{bp-a}}\right)[-h_{r,ap-bp}(T_{ap} - Tf2{+}Ubp{-}aTf2{-}Ta \quad (8)$$

$$T_{ap} - T_{f2} = -\left(\frac{U_T+U_B+h_{c,ap-f1}}{U_T+U_B+h_{c,ap-f1}+h_{c,ap-f2}}\right)(T_{f2} - T_a) + \left(\frac{h_{c,ap-f1}}{U_T+U_B+h_{c,ap-f1}+h_{c,ap-f2}}\right)(T_{f1} - T_a) + \left(\frac{I\alpha_{ap}\tau_{gc}^2}{U_T+U_B+h_{c,ap-f1}+h_{c,ap-f2}}\right) \quad (9)$$

$$T_{ap} - T_{f2} = -J_5(T_{f2} - T_a) + J_6(T_{f1} - T_a) + J_3 \quad (10)$$

Putting the expression $(T_{ap} - T_{f2})$ from Equation 10 into Equation 8, we have

$$T_{f2} - T_{bp} = J_7[(U_{bp-a} + J_5h_{r,ap-bp})(T_{f2} - T_a) - J6hr,ap{-}bpTf1{-}Ta{-}J3hr,ap{-}bp \quad (11)$$

Assume the differential length dx at a distance x from the inlet of the collector.

For flow 1 (air flowing over the absorbing plate),

$$h_{c,ap-f1}(T_{ap}-T_{f1})=\left(\frac{m\varphi c_p}{W}\right)\left(\frac{dT_{f1}}{dx}\right)+h_{c,f1-gc1}(T_{f1}-Tgc1 \quad (12)$$

Substituting the expressions of $(T_{ap}-T_{f1})$ from Equation 5 and $(T_{f1}-T_{gc1})$ from Equation 6 into Equation 12, we have

$$\frac{Z\varphi d\,(T_{f1}-T_a)}{d\zeta}=M_1(T_{f1}-T_a)+M_2(T_{f2}-T_a)+M_3 \quad (13)$$

For flow 2 (air flowing under the absorbing plate),

$$h_{c,ap-f2}(T_{ap}-T_{f2})=\left[\frac{m(1-\varphi)c_p}{W}\right]\left(\frac{dT_{f2}}{dx}\right)+h_{c,f2-bp}(T_{f2}-T_{bp}) \quad (14)$$

Substituting the expressions of $(T_{ap}-T_{f2})$ from Equation 10 and $(T_{f2}-T_{bp})$ from Equation 11 into Equation 14, we have

$$\frac{Z(1-\varphi)d(T_{f2}-T_a)}{d\zeta}=M_4(T_{f1}-T_a)+M_5(T_{f2}-T_a)+M_6 \quad (15)$$

Where, $Z=\frac{mc_p}{WL}=\frac{mc_p}{A_c}$

$$\zeta=\frac{x}{L}$$

All the coefficients J's and M's (given in Appendix A) are in terms of the convective heat transfer coefficient, loss coefficients and physical properties.

Solving Equations 13 and 15 with the boundary condition:

At, $\zeta=0, T_{f1}=T_{f2}=T_{f,i}$

The temperature distributions of flow 1 and flow 2 as

$$T_{f1}=\left[\frac{Y_1-\frac{M_5}{1-\varphi}}{\frac{M_4}{(1-\varphi)}}\right]C_1e^{\frac{Y_1}{Z}\zeta}+\left[\frac{Y_2-\frac{M_5}{1-\varphi}}{\frac{M_4}{(1-\varphi)}}\right]C_2e^{\frac{Y_2}{Z}\zeta}-\frac{M_5}{M_4}\left(\frac{M_3M_4-M_1M_6}{M_1M_5-M_2M_4}\right)-\frac{M_6}{M_4}+T_a \quad (16)$$

$$T_{f2}=C_1e^{\frac{Y_1}{Z}\zeta}+C_2e^{\frac{Y_2}{Z}\zeta}+\frac{M_3M_4-M_1M_6}{M_1M_5-M_2M_4}+T_a \quad (17)$$

The outlet temperature of flow 1, can be obtained from Equation 16, for, $\zeta=1, T_{f1}=T_{f1,o}$

$$T_{f1,o}=\left[\frac{Y_1-\frac{M_5}{1-\varphi}}{\frac{M_4}{(1-\varphi)}}\right]C_1e^{\frac{Y_1}{Z}}+\left[\frac{Y_2-\frac{M_5}{1-\varphi}}{\frac{M_4}{(1-\varphi)}}\right]C_2e^{\frac{Y_2}{Z}}-\frac{M_5}{M_4}\left(\frac{M_3M_4-M_1M_6}{M_1M_5-M_2M_4}\right)-\frac{M_6}{M_4}+T_a \quad (18)$$

The outlet temperature of flow 2, can be obtained from Equation 17, for, $\zeta=1, T_{f2}=T_{f2,o}$

$$T_{f2,o}=C_1e^{\frac{Y_1}{Z}}+C_2e^{\frac{Y_2}{Z}}+\frac{M_3M_4-M_1M_6}{M_1M_5-M_2M_4}+T_a \quad (19)$$

For Y_1, Y_2, C_1 and C_2 referred to Appendix A.

The useful energy gain by the flow 1 and flow 2 are, respectively

$$Q_{uf1}=m\varphi c_p(T_{f1,o}-T_{f,in})=Z\varphi A_c(T_{f1,o}-T_{f,in}) \quad (20)$$

$$Q_{uf2}=m(1-\varphi)c_p(T_{f2,o}-T_{f,in})=Z(1-\varphi)A_c(T_{f2,o}-T_{f,in}) \quad (21)$$

The total energy gain is

$$Q_{uf}=Q_{uf1}+Q_{uf2} \quad (22)$$

The collector efficiency is

$$\eta=\frac{Q_{uf}}{A_cI}=\frac{Z}{I}\left[\varphi T_{f1,o}+(1-\varphi)T_{f2,o}-T_{f,in}\right] \quad (23)$$

$$\eta=\frac{mc_p}{IA_c}(T_{f,o}-T_{f,in})=\frac{Z}{I}\Delta T \quad (24)$$

2.2 Heat Transfer Coefficients

Figure 2 shows the thermal network of double glass double flow solar air heater. The resistances to energy loss through the bottom and edges of the collector and from the surfaces of the bottom and edges of the collector to the ambient are mainly the resistance to heat flow through the insulation by conduction,

$$U_{bp-a}\approx\frac{k}{l} \quad (25)$$

and

$$\frac{1}{U_B}=\frac{1}{U_{bp-a}}+\frac{1}{h_{c,f2-bp}}+\frac{l_{bp}}{k_{bp}} \quad (26)$$

The thermal resistance from inner glass cover through outer glass cover to the ambient, may be expressed as

$$\frac{1}{U_{gc1-a}}=\frac{1}{h_w+h_{r,gc2-a}}+\frac{1}{h_{c,gc1-gc2}+h_{r,gc1-gc2}} \quad (27)$$

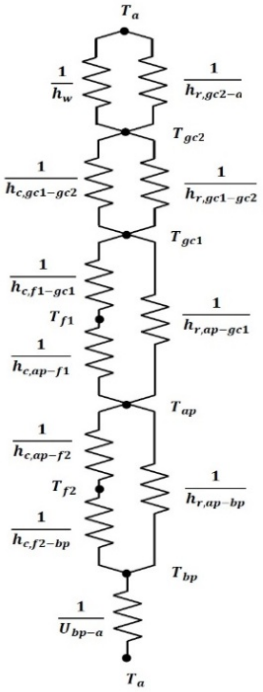

Fig. 2. Thermal network of double glass double flow solar air heater.

An empirical equation, derived by Klein [20], is used to calculate top loss coefficient, U_T, and is given by

$$U_T = \left[\frac{2(T_{ap,m}/520)}{\left\{\frac{(T_{ap,m}-T_a)}{\{2+(1+0.089h_w-0.1166h_w\varepsilon_{ap})(1+0.07866\times2)\}}\right\}^{0.43(1-100/T_{ap,m})}} + \frac{1}{h_w}\right]^{-1} + \frac{\sigma(T_{ap,m}+T_a)(T_{ap,m}^2+T_a^2)}{\left[(\varepsilon_{ap}+2\times0.00591h_w)^{-1}+\{2\times2+(1+0.089h_w-0.1166h_w\varepsilon_{ap})(1+0.07866\times2)-1+0.133\varepsilon_{ap}\}/\varepsilon_{gc}-2\right]} \quad (28)$$

The convective heat transfer coefficients between the absorbing plate and air flow 1 is assumed to be equal to the convective heat transfer coefficient between air flow 1 and inner glass cover, and the convective heat transfer coefficients between the absorbing plate and air flow 2 is assumed to be equal to the convective heat transfer coefficient between air flow 2 and bottom plate.

$$h_{c,ap-f1} = h_{c,f1-gc1} \quad (29)$$

and, $h_{c,ap-f2} = h_{c,f2-bp}$ (30)

The convective heat transfer coefficient from the outer glass cover (gc2) due to wind is calculated by the expression given by McAdams [21].

$$h_w = 5.7 + 3.8V \quad (31)$$

The heat transfer coefficient between two glass covers, inner glass cover (gc1) and outer glass cover (gc2) is expressed by Hottel and Woertz [22] empirical equation as

$$h_{c,gc1-gc2} = 1.25\left(T_{gc1,m} - T_{gc2,m}\right)^{0.25} \quad (32)$$

The radiative heat transfer coefficients between the absorbing plate and inner glass cover and between the absorbing plate and bottom plate may be expressed by assuming mean radiant temperature equal to the mean fluid temperature as [3].

$$h_{r,ap-gc1} \approx \frac{4\sigma T_{f1,m}^3}{\frac{1}{\varepsilon_{ap}}+\frac{1}{\varepsilon_{gc1}}-1} \quad (33)$$

and

$$h_{r,ap-bp} \approx \frac{4\sigma T_{f2,m}^3}{\frac{1}{\varepsilon_{ap}}+\frac{1}{\varepsilon_{bp}}-1} \quad (34)$$

The radiative heat transfer coefficients between the two glass cover inner glass cover and outer glass cover and outer glass cover and air are respectively,

$$h_{r,gc1-gc2} = \frac{\sigma(T_{gc1,m}^2+T_{gc2,m}^2)(T_{gc1,m}+T_{gc2,m})}{\frac{1}{\varepsilon_{gc1}}+\frac{1}{\varepsilon_{gc2}}-1} \quad (35)$$

and

$$h_{r,gc2-a} = \varepsilon_{gc2}\sigma(T_{gc2,m}^2 + T_a^2)(T_{gc2,m} + T_a) \quad (36)$$

Assuming the heat transfer coefficients between fluid and duct walls equal,

$$h_{c,ap-f1} = h_{c,f1-gc1} \text{and} h_{c,ap-f2} = h_{c,f2-bp} \quad (37)$$

For flat plate absorber, the convective heat transfer coefficient for air is,

$$h_{c,ap-f1} = \frac{Nu_1 k_{f1}}{D_{h1}} \quad (38)$$

$$h_{c,ap-f2} = \frac{Nu_2 k_{f2}}{D_{h2}} \quad (39)$$

For laminar flow, the equation presented by Heaton *et al.* [23],

$$Nu_i = 4.4 + \frac{0.00398\,(0.7Re_iD_{hi}/L)^{1.66}}{1+0.0114\,(0.7Re_iD_{hi}/L)^{1.12}} \quad (40)$$

For turbulent flow the correlation derived from Kays [24], data with the modification of McAdams [21],

$$Nu_i = 0.0158Re_i^{0.8}[1 + (D_{hi}/L)^{0.7}] \quad (41)$$

Where $i = 1, 2$ (for flow 1, flow 2)

The hydraulic diameter of the duct

$$D_{hi} = \frac{4WH_c}{2(W+H_c)} \quad (42)$$

Reynolds number for upper duct,

$$Re_1 = \frac{D_{h1}V_{f1}\rho_{f1}}{\mu_{f1}} = \frac{[4WH/2(W+H)][m\varphi/(\rho_{f1}WH)]\rho_{f1}}{\mu_{f1}} = \frac{2m\varphi}{\mu_{f1}(W+H)} \quad (43)$$

and, Reynolds number for lower duct,

$$Re_2 = \frac{D_{h2}V_{f2}\rho_{f2}}{\mu_{f2}} = \frac{2m(1-\varphi)}{\mu_{f2}(W+H)} \quad (44)$$

For v-corrugated absorber, the construction of the corrugated plate solar air heater (Figure 3) is similar to the flat plate solar air heater except the absorber plate is replaced by v-corrugated shape. The energy balance equations are same only heat transfer coefficient between absorber plate and flowing fluid are different. The developed area of the corrugated plate is greater than the flat plate by a factor of $1/sin(\theta/2)$ [25] thus the heat transfer coefficient between absorbing plate to fluid is

$$h_{c,ap-f1} = \frac{Nu_1 k_{f1}}{D_{h1}} \times \frac{1}{sin\left(\frac{\theta}{2}\right)} \quad (45)$$

$$h_{c,ap-f2} = \frac{Nu_2 k_{f2}}{D_{h2}} \times \frac{1}{sin\left(\frac{\theta}{2}\right)} \quad (46)$$

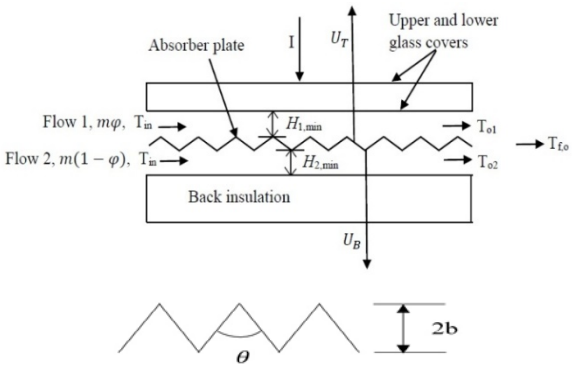

Fig. 3. The double flow v-corrugated absorber solar air heater.

The approximated hydraulic diameter of the duct

$$D_{hi} = H_{i,min} + b \quad (47)$$

Karim *et al.* [25] modified the Hollands and Shewen [26] correlation of Nusselts number (Nu) as:
If $Re < 2800$

$$Nu = 2.821 + 0.126\,Re\frac{2b}{L} \quad (48)$$

If $2800 \leq Re \leq 10^4$

$$Nu = 1.9 \times 10^{-6} Re^{1.79} + 225 \frac{2b}{L} \quad (49)$$

If $10^4 \leq Re \leq 10^5$

$$Nu = 0.0302 Re^{0.74} + 0.242 Re^{0.74} \frac{2b}{L} \quad (50)$$

2.3 Mean Temperature

The mean air temperatures in the ducts can be found by integrating Equations 16 and 17 from $\zeta = 0$ to $\zeta = 1$, and the expressions are:

$$T_{f1,m} = \left[\frac{Y_1 - \frac{M_5}{1-\varphi}}{\frac{M_4}{(1-\varphi)}}\right] C_1 \frac{Z}{Y_1} e^{\left(\frac{Y_1}{Z}-1\right)} + \left[\frac{Y_2 - \frac{M_5}{1-\varphi}}{\frac{M_4}{(1-\varphi)}}\right] C_2 \frac{Z}{Y_2} e^{\left(\frac{Y_2}{Z}-1\right)} - \frac{M_5}{M_4}\left(\frac{M_3 M_4 - M_1 M_6}{M_1 M_5 - M_2 M_4}\right) - \frac{M_6}{M_4} + T_a \quad (51)$$

$$T_{f2,m} = C_1 \frac{Z}{Y_1} e^{\left(\frac{Y_1}{Z}-1\right)} + C_2 \frac{Z}{Y_2} e^{\left(\frac{Y_2}{Z}-1\right)} + \frac{M_3 M_4 - M_1 M_6}{M_1 M_5 - M_2 M_4} + T_a \quad (52)$$

The overall loss coefficient is the sum of top and bottom loss coefficients:

$$U_L = U_T + U_B \quad (53)$$

The mean absorbing plate temperature can be calculated by

$$T_{ap,m} = \frac{I\alpha_{ap}\tau_{gc}^2 + U_L T_a + h_{c,ap-f1} T_{f1,m} + h_{c,ap-f2} T_{f2,m}}{U_L + h_{c,ap-f1} + h_{c,ap-f2}} \quad (54)$$

The mean temperature of inner glass cover (gc1)

$$T_{gc1,m} = \frac{U_{gc1-a} T_a + h_{r,ap-gc1} T_{ap,m} + h_{c,f1-gc1} T_{f1,m}}{U_{gc1-a} + h_{r,ap-gc1} + h_{c,f1-gc1}} \quad (55)$$

The mean temperature of outer glass cover (gc2)

$$T_{gc2,m} = \frac{(h_{c,gc1-gc2} + h_{r,gc1-gc2}) T_{gc1,m} + h_w T_a}{h_{c,gc1-gc2} + h_{r,gc1-gc2} + h_w} \quad (56)$$

2.4 Thermohydraulic (Effective) Efficiency

The net energy gain, Q_e, of the collector can be expressed as the difference between the useful thermal energy gain, Q_{uf}, and the equivalent thermal energy required for producing the work energy necessary to overcome the pressure energy losses [27]. This net energy can be written as:

$$Q_e = Q_{uf} - P_m / C_f \quad (57)$$

Where P_m is the work energy lost in friction in the heater channel, given by:

$$P_m = m\Delta P / \rho \quad (58)$$

C_f is the conversion factor to transform different efficiencies (thermal to mechanical) and is taken 0.2 [28].

The pressure drop ΔP is calculated from the following expression;

$$\Delta P = \Delta P_{ch} + \Delta P_{en} + \Delta P_{ex} \quad (59)$$

The pressure drop through the upper and lower channel ΔP_{ch} is calculated by the relation [29-31];

$$\Delta P_{ch} = 2\rho v_{ch}^2 f L / D_{hi} \quad (60)$$

Hydraulic diameter for flat plate (smooth channel) solar air heater;

$$D_{hi} = 2H_c W / (H_c + W) \quad (61)$$

Hydraulic diameter for v-corrugated absorber solar air heater;

$$D_{hi} = 2H_c W / (H_c + W) \times sin(\theta/2) \quad (62)$$

The friction factor is given by [29-32];
For turbulent flow,

$$f = 0.059 Re^{-0.2} \quad (63)$$

for laminar flow

$$f = 16/Re \quad (64)$$

The sum of the inlet and outlet pressure drop ($\Delta P_{en} + \Delta P_{ex}$) can be determined by Hegazy [33];

$$\Delta P_{en} + \Delta P_{ex} = (R_{en} + R_{ex}) \frac{\rho v_p^2}{2} \quad (65)$$

Where the sum of the entrance and exit resistance factor ($R_{en} + R_{ex}$) is taken 1.5 [34].

The thermohydraulic (effective) efficiency of the solar air heater can be expressed as;

$$\eta_{eff} = \frac{Q_e}{A_c I} = \frac{Q_{uf} - (P_m / C_f)}{A_c I} \quad (66)$$

3. CALCULATION METHOD

For performing the numerical calculations of this study a computer program in C++ language was developed considering the following system, operating and metrological parameters:
L = 1.25 m, W = 0.80 m, H_{gc} = 0.025 m, H_c = 0.025 m, τ_{gc} = 0.875, α_{ap} = 0.96, ε_{gc} = 0.94, ε_{ap} = 0.80, ε_{bp} = 0.94, $U_B \approx 0$, T_a = 30 °C = 303 K, V = 1 m/s, b = 0.01 m, I = 1000W/m^2, m = 0.014 – 0.083 kg/s, φ = 0.2, 0.4, 0.5, 0.6 and 0.8.

The physical properties including density, specific heat, the dynamic viscosity and the thermal conductivity of air have been taken at mean temperature.

The procedure followed for determination of thermal and thermo hydraulic performance briefly explained as,

(i) First assumed the values of $T_{f1,m}$, $T_{f2,m}$, $T_{ap,m}$, $T_{gc1,m}$ and $T_{gc2,m}$.
(ii) By using assumed values and using Equations 32 to 39; calculate the heat transfer coefficients.
(iii) To check the assumed temperature values $T_{f1,m}$, $T_{f2,m}$, $T_{ap,m}$, $T_{gc1,m}$ and $T_{gc2,m}$ use Equations 51 to 56 and obtained new temperature values. If the calculated values of temperatures are different from the assumed values continued calculation by iteration method. These new temperatures will be use as the assumed temperatures for next iteration and the process will be repeated until all the newest temperatures obtained are their respective previous values.

(iv) After completing the iteration the mean temperature values were obtained and energy gain and thermal efficiency can be calculated by Equations 22 and 23.

(v) By using Equation 59 calculate pressure drop including channel pressure drop, entrance and exit pressure drop, then calculate net energy gain and thermo hydraulic efficiency by Equations 57 and 66, respectively.

4. RESULTS AND DISCUSSION

The results of performance parameters have been obtained analytically for various values of system and operating parameters for double flow flat plate and v-corrugated absorbers with different v-angle (θ). These results have been plotted to analyse the thermal and thermo hydraulic performance of different type of double flow v-corrugated absorber solar air heaters and results are compared with conventional solar air heater.

Figure 4 shows the plot of air temperature rise as a function of the fraction of mass flow rates (φ) for double flow flat plate and v-corrugated absorber solar air heater with different v-groove angles at mass flow rate (m) of 0.014 kg/s. It is seen from the figure that the air temperature rise increases with increase in fraction of mass flow rate up to φ = 0.5, then there after rise in air temperature decreases with increasing the value of 'φ'. This type of trend is observed due to fact that for φ > 0.5, the heat losses increases because of gradual increase in mass flow rate through the upper channel. From the figure it is also seen that there is a significant gain in air temperature rise by v-corrugated absorber collector with respect to flat plate collector. It is clearly seen from the figure that the double flow solar air heater having 60° v-angle maintains highest air temperature rise at all values of φ.

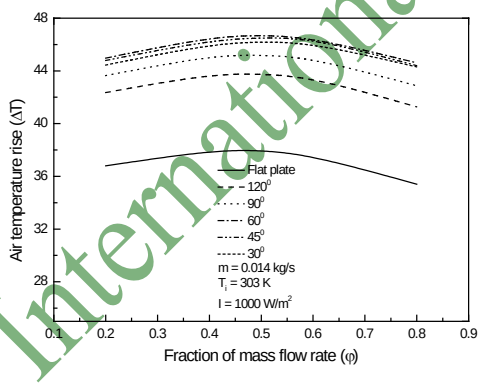

Fig. 4. Air temperature rise vs. fraction of mass flow rate.

Figure 5 shows the variation of efficiency for different angle of v-corrugated absorbers solar air heater with fraction of mass flow rate for m = 0.014 kg/s. It is evident that the efficiency increases with increase in fraction of mass flow rate and reaches its peak value at φ = 0.5 and then it decreases gradually with increasing the value of 'φ'. This characteristic behaviour appears due to fact that beyond φ > 0.5, loses from top increases due to increased amount of air mass flow rate through upper channel. As seen from the figure, the absorber with 60° v-angle depicts highest efficiency values among all other different angle of v-corrugated absorbers at all values of fraction of mass flow rate.

The air temperature rise and efficiency values for flat and different angle of v-corrugated double flow solar air heaters are shown in Table 1 for three different mass flow rates. Inspection of table indicates that air temperature rise and efficiency increases with increase in 'φ', attains the maximum values at φ = 0.5 (i.e. at equal air mass flow rate through both channels), then there after it decreases gradually as it reaches at φ = 0.8. Such type of results is obvious due to enhance rate of heat losses from absorbers to surroundings, when air is flowing through the upper channel is high.

Result clearly indicate that the air temperature rise and efficiency increases with increase in v-groove angle (θ), attains maximum values when θ = 60°, then there after it decreases. Results also indicate that there is an improvement in thermal performance by replacing flat plate to v-corrugated absorber in double flow solar air heater. The efficiency of double flow v-corrugated absorber solar air heater is 61.58 % to 65.73 % at lower mass flow rate of 0.014 kg/s and 77.74 % to 78.53 % for higher mass flow rate of 0.083 kg/s for φ = 0.5.

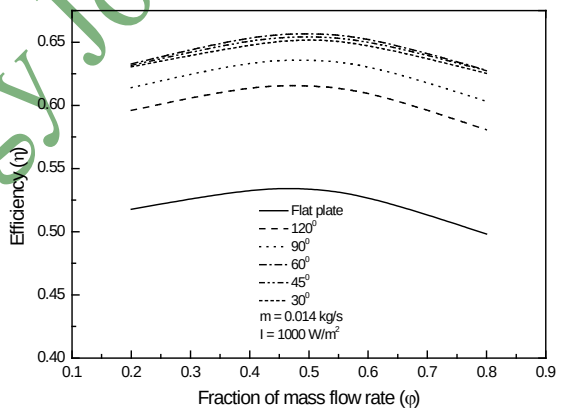

Fig. 5. Efficiency vs. fraction of mass flow rate.

Figure 6 illustrate the variation of air temperature rise for flat plate and different angle of v-corrugated absorber solar air heaters with mass flow rate for φ = 0.5. Figure reveals that the air temperature rise decreases with increase in mass flow rate for all types of absorbers. It is clearly seen from the figure that the considerable amount of gain in air temperature rise at lower mass flow rate is observed due to corrugated absorber and gain in air temperature rise drastically decreases at higher mass flow rate. This type of results is expected due to approaching equality of absorber and air temperature at higher mass flow rate.

Figure 7 which shows the plot of efficiency as a function of mass flow rate (when φ = 0.5) for a set of system parameters; reveal that the efficiency monotonically increases with increase in mass flow rate apparently because of an increase in thermal conductance; furthermore, a slight fall is observed in the rate of increase of efficiency as mass flow rate increases apparently due to lower percentage increase in surface

conductance as mass flow rate increases. The 60˚ v-angle absorber, maintains the highest efficiency value throughout the range of mass flow rates investigated. It is also observed from the figure that at lower mass flow rate the efficiency of 45˚ and 30˚ v-corrugated absorber solar air heater are higher than 90˚ and 120˚ angle absorber, however, as mass flow rate increases the efficiency of 45˚ and 30˚ angle absorber decreases due to flow separation and formation of vortices.

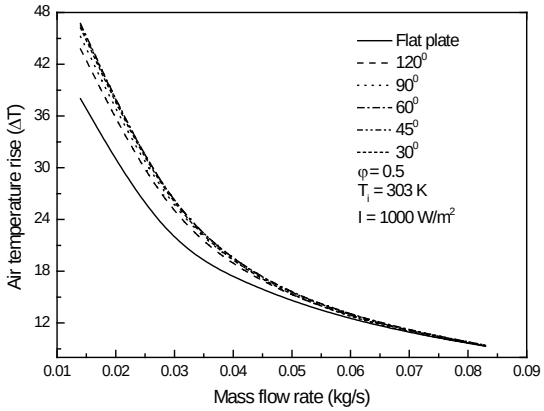

Fig. 6. Air temperature rise vs. mass flow rate.

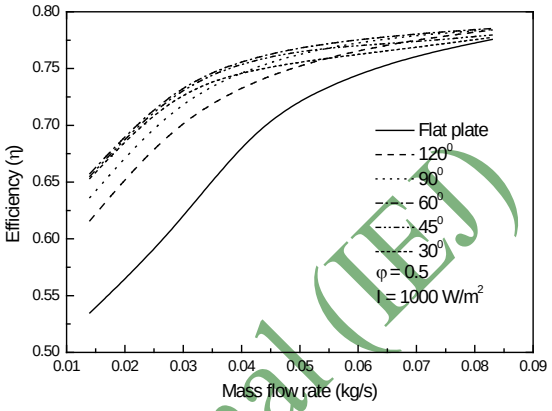

Fig. 7. Efficiency vs. mass flow rate.

Table 1. The air temperature rise and efficiency for flat plate and different angles of v-corrugated double flow solar air heaters.

Mass flow rate (kg/s)	Fraction of mass flow rate (φ)	Air temperature rise, ΔT (˚C)						Efficiency (%)					
		Flat plate	120˚	90˚	60˚	45˚	30˚	Flat plate	120˚	90˚	60˚	45˚	30˚
0.014	0.2	36.79	42.36	43.63	44.97	44.79	44.44	51.77	59.60	61.40	63.27	63.16	63.04
	0.4	37.96	43.76	45.15	46.56	46.32	46.03	53.42	61.57	63.53	65.52	65.25	64.85
	0.5	38.01	43.77	45.22	46.72	46.52	46.22	53.47	61.58	63.63	65.73	65.51	65.31
	0.6	37.58	43.50	44.98	46.52	46.47	46.11	52.87	61.20	63.29	65.46	65.19	64.87
	0.8	35.41	41.27	42.86	44.62	44.40	44.31	49.82	58.07	60.31	62.77	62.73	62.53
0.055	0.2	13.08	13.28	13.51	13.67	13.45	13.20	72.30	73.42	74.68	75.56	74.45	73.24
	0.4	13.29	13.73	13.88	13.94	13.86	13.67	73.50	75.89	76.76	77.07	76.65	75.57
	0.5	13.32	13.76	13.92	13.98	13.91	13.70	73.64	76.06	76.94	77.28	76.87	75.94
	0.6	13.28	13.75	13.91	13.98	13.90	13.70	73.44	76.03	76.93	77.28	76.87	75.74
	0.8	12.97	13.34	13.61	13.82	13.52	13.27	71.68	73.77	75.27	76.40	75.09	73.59
0.083	0.2	9.03	9.20	9.25	9.26	9.18	9.05	75.38	76.75	77.13	77.16	76.63	75.54
	0.4	9.27	9.34	9.38	9.39	9.30	9.28	77.34	77.84	78.10	78.24	77.65	77.44
	0.5	9.29	9.39	9.40	9.41	9.34	9.30	77.57	78.38	78.43	78.53	77.95	77.74
	0.6	9.28	9.34	9.37	9.38	9.31	9.29	77.38	77.96	78.15	78.22	77.70	77.42
	0.8	9.02	9.26	9.33	9.33	9.23	9.12	75.31	77.29	77.77	77.85	77.19	76.14

The efficiency, enhancement in efficiency of double flow solar air heaters of different angle of v-corrugated absorber with respect to conventional and flat plate double flow solar air heater (at φ = 0.5) for three different mass flow rate of 0.014, 0.055 and 0.083 kg/s are tabulated in Table 2. Comparison of the results of the double flow v-corrugated absorbers solar air heater of different v-angle solar air heaters with flat plate solar air heater show a substantial enhancement in efficiency. It has been observed from the table that the rate of enhancement in efficiency of v-corrugated absorbers is more pronounced at lower mass flow rate than higher mass flow rate lower mass flow rate of 0.014 kg/s. This corresponds to. The efficiency increases from 61.58 % to 65.73 % as angle of v-corrugated absorber vary from 30˚ to 120˚ at 15.16 % to 22.93 % enhancement in efficiency as compared to flat plate double flow solar air heater. Results also show that the highest percentage enhancement in efficiency of double flow 60˚ v-corrugated absorber solar air heater at lower mass flow rate of 0.014 kg/s is found to be 171.17% over conventional plane solar air heater and 22.93% for double flow flat plate solar air heater and these values are 54.58 % and 1.23 % respectively for highest mass flow rate of 0.083 kg/s.

Table 2. Efficiency and enhancement in efficiencies for double flow solar air heater for different angle of v-corrugated absorber for φ = 0.5.

Mass flow rate (kg/s)		C_{SAH}	Flat plate	120˚	90˚	60˚	45˚	30˚
0.014	η	24.23	53.47	61.58	63.63	65.73	65.51	65.31
	$E_{\eta C}$ (%)	_	120.68	154.15	162.61	171.17	170.36	169.54
	$E_{\eta FP}$ (%)	_	_	15.16	19.00	22.93	22.52	22.14
0.055	η	44.83	73.64	76.06	76.94	77.28	76.87	75.94
	$E_{\eta C}$ (%)	_	64.26	69.66	71.62	72.38	71.47	69.39
	$E_{\eta FP}$ (%)	_	_	3.28	4.48	4.94	4.38	3.12
0.083	η	50.80	77.57	78.38	78.43	78.53	77.95	77.74
	$E_{\eta C}$ (%)	_	52.69	54.29	54.39	54.58	53.44	53.03
	$E_{\eta FP}$ (%)	_	_	1.04	1.11	1.23	0.49	0.22

C_{SAH}: Conventional solar air heater.
$E_{\eta C}$: Enhancement in efficiency with respect to C_{SAH}.
$E_{\eta FP}$: Enhancement in efficiency with respect to double flow flat plate solar air heater.

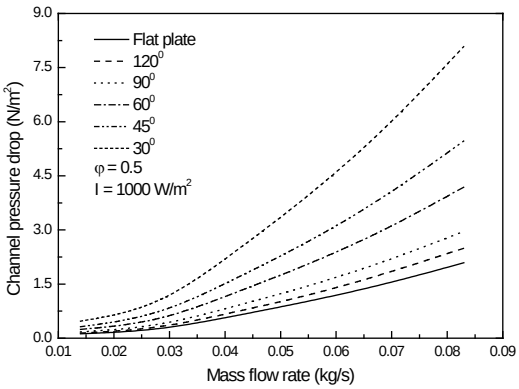

Fig. 8. Channel pressure drop vs. mass flow rate.

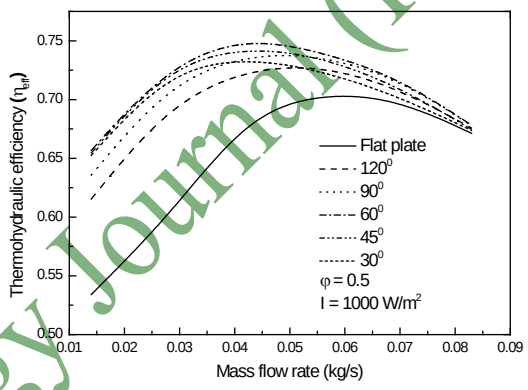

Fig. 9. Thermohydraulic efficiency vs. mass flow rate.

The effect of mass flow rate on the channel pressure drop is shown in Figure 8. It is clearly seen from figure that, the pressure drop increases with increase in mass flow rate. This is because of fact that increase in mass flow rate increases the velocity of air leading to higher pressure drop. It is seen that the v-corrugated absorbers have higher pressure drop as compared to flat plate collector because of increased friction. The 30˚ v-corrugated air heater shows the highest pressure drop, this is probably due to increased surface area causes increased resistance during air flow.

Figure 9 shows the thermohydraulic efficiency as a function of mass flow rate of air for flat plate and various angle of v-corrugated absorber solar air heaters. It is seen from the plot that the thermohydraulic efficiency increases with increase in mass flow rate up to a critical value of flow rate at which it attains a maximum value and subsequently decreases for all collectors. Results indicate that thermohydraulic efficiency of double flow flat plate solar air heater reaches maximum value at m = 0.062 kg/s whereas for other collectors pick values of thermohydraulic efficiency shifted towards lower mass flow rates. This type of trends is observed due to increase in pressure drop of flowing air in case of corrugated absorber. Again most efficient 60˚ v-corrugated double flow solar air heater attains maximum value of thermohydraulic efficiency at m = 0.045 kg/s.

5. MATHEMATICAL MODEL VALIDATION

The present mathematical models of solar air heaters have been compared with the experimental values obtained from Ho-Ming Yeh *et al.* [3] and El Sebaii *et al.* [11]. Figure 10 shows the comparison of analytical and experimental values of efficiency with fraction of mass flow rate. The maximum deviation of analytical values of efficiency is 2.27 % from the experimental values of Ho-Ming Yeh *et al.* [3]. Figure 11 shows the comparison of analytical with experimental values of thermal efficiency of El Sebaii *et al.* [11] of double flow flat plate and 60˚ v-corrugated absorber solar air heater. The maximum deviation in efficiency for flat plate and 60˚ v-corrugated collectors are found to be ±5.47 % and 4.46 % respectively. This shows good resemblance of analytical and experimental values which makes validation of calculated numerical data with present mathematical modelling.

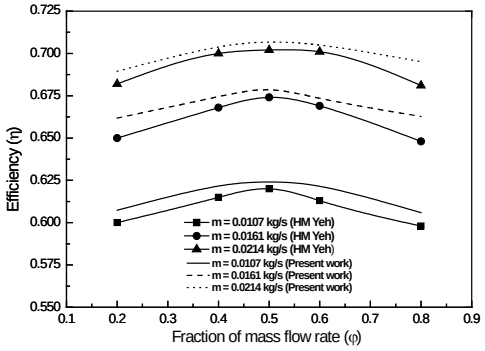

Fig. 10. Comparison of analytical efficiency data with available experimental data Ho-Ming Yeh [3].

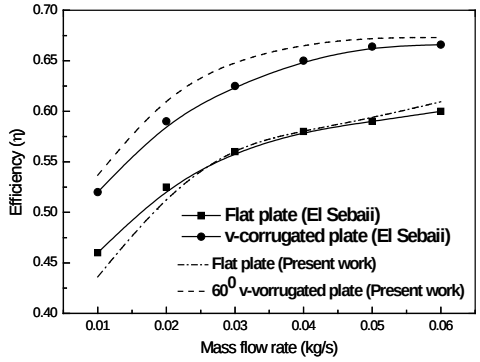

Fig. 11. Comparison of analytical efficiency data with available experimental data of El Sebaii [11].

6. CONCLUSIONS

On the basis of above results the following conclusions are drawn:

(i) The mathematical model for double flow solar air heater have been developed to study the effect of mass flow rate, fraction of mass flow rate and angle of v-corrugated absorber on the thermal and thermohydraulic performance of collector.

(ii) A computer program in C++ language has been developed to solve the mathematical model and obtained the results of air temperature rise, efficiency, pressure drop and effective efficiency to analyze the effect of system and operating parameters.

(iii) The mass flow rate should be equal in both flow channel of double flow solar air heater i.e. fraction of mass flow rate is 0.5, for the best thermal and thermohydraulic performance.

(iv) It is observed that efficiency increases with increase in mass flow rate but effective efficiency increases upto a certain limit of mass flow rate and there after it decreases.

(v) All v-corrugated absorber double flow collectors have perform better than flat plate collector. However, among all v-corrugated absorber, 60˚ angle v-corrugated absorber collector have the best thermal and thermohydraulic performance.

(vi) The analytical and experimental values of thermal efficiency have been found to compare reasonably well in the range of parameters investigated. The percentage deviation in efficiency of double flow flat plate and 60˚ v-corrugated absorber solar air heater is found to be in the range of ± 5.47 % and 4.46 % respectively.

NOMENCLATURE

A_c area of collector (m^2)
b half height of v-groove (m)
C_p specific heat of air at constant pressure (J/kg K)
D_h hydraulic diameter (m)
f friction coefficient
h convective heat transfer coefficient (W/m^2 K)
H_c average height of air flow channel (m)
H_{gc} height of glass cover (m)
I insolation (W/m^2)
k thermal conductivity (W/m K)
L collector length (m)
l thickness (m)
m mass flow rate (kg/s)
Nu Nusselt number
Q energy gain by air (W)
R resistance factor
Re Reynolds number
T temperature (K)
U loss coefficient (W/m^2 K)
V velocity of wind (m/s)
v velocity of air (m/s)
W collector width (m)

Greek symbols

α absorptivity
ε emissivity
φ fraction of mass flow rate
ΔP pressure drop (N/m^2)
η efficiency
μ viscosity of air (Ns/m^2)
ρ density of air (kg/m^3)
σ Stefan-Boltzmann constant (W/m^2 K^4)
τ transmissivity
θ angle of v-groove absorbing plate (˚)

Subscripts

a ambient
ap absorber plate
B bottom
bp bottom plate
c convective
ch channel
e net
en entrance
ex exit
f total flow
$f1$ flow above the absorber plate
$f2$ flow under the absorber plate
gc glass cover
$gc1$ lower glass cover
$gc2$ upper glass cover
in inlet

L overall
m mean
max maximum
min minimum
o outlet
r radiative
T top
eff thermohydraulic (effective)
u useful
w wind
1 duct above the absorber plate
2 duct under the absorber plate

REFERENCES

[1] Goldstein L. and E.M. Sparrow. 1976. Experiments on the transfer characteristics of a corrugated fin and tube heat exchanger configuration. *Transaction of the ASME, Journal of Heat Transfer* 98: 26-34.

[2] Goldstein L. and E.M. Sparrow. 1977. Heat/mass transfer characteristics for flow in a corrugated wall channel. *Transaction of the ASME, Journal of Heat Transfer* 99: 187-195.

[3] Yeh H.-M., Ho C.-D. and Hou J.-Z. 1999. The improvement of collector efficiency in solar air heaters by simultaneously air flow over and under the absorbing plate. *Energy* 24: 857-871.

[4] Hikmet E., 2008. Experimental energy and exergy analysis of a double flow solar air heater having different obstacles on absorber plates. *Building and Environment* 43: 1046-1054.

[5] Mohammadi K. and M. Sabzpooshani. 2013. Comprehensive performance evaluation and parametric studies of single pass air heater with fins and baffles attached over the absorber plate. *Energy* 57: 741-750.

[6] Fakoor P.M., Lashkari A., Tabrizi H., Basirat and Hosseini R., 2011. Performance evaluation of a natural convection solar air heater with a rectangular finned absorber plate. *Energy Conversion and Management* 52: 1215-1225.

[7] Priyam A. and P. Chand. 2016. Thermal and thermohydraulic performance of wavy finned absorber solar air heater. *Solar Energy* 130: 250-259.

[8] Mittal M.K., Varun, Saini R.P. and Singal S.K., 2007. Effective efficiency of solar air heaters having different types of roughness element on the absorber plate. *Energy* 32: 739-745.

[9] Naphon P., 2005. Effect of porous media on the performance of the double pass flat plate solar air heater. *International Communications in Heat and Mass Transfer* 32: 140-150.

[10] Vimal K., Chouksey and Sharma S.P., 2016. Investigations on thermal performance characteristic of wire screen packed bed solar air heater. *Solar Energy* 132: 591-605.

[11] Taymaz I., Koc I. and Islamoglu Y., 2008. Experimental study on forced convection heat transfer characteristics in a converging diverging heat exchanger channel. *Heat Mass Transfer* 44: 1257-1262.

[12] Hamza A., Ali H. and Hanaoka Y., 2002. Experimental study on laminar flow forced convection in a channel with upper V-corrugated plate heated by radiation. *International Journal of Heat and Mass Transfer* 45: 2107-2117.

[13] Fabbri G., 2000. Heat transfer optimization in corrugated wall channels. *International Journal of Heat and Mass Transfer* 43: 4299-4310.

[14] Naphon P., 2007. Heat transfer characteristics and pressure drop in channel with V-corrugated upper and lower plates. *Energy Conversion and Management* 48: 1516-1524.

[15] El-Sebaii A.A., Aboul-Enein S., Ramadan M.R.I., Shalaby S.M. and Moharram B.M., 2011. Investigation of thermal performance of double pass flat and v-corrugated plate solar air heaters. *Energy* 36: 1076-1086.

[16] Wenxian L., Wenfeng G. and Tao L., 2006. A parametric study on the thermal performance of cross corrugated solar air collectors. *Applied Thermal Engineering* 26: 1043-53.

[17] Wenfeng G., Wenxian L., Tao L. and Chaofeng, X., 2007. Analytical and experimental studies on the thermal performance of cross corrugated and flat pate solar air heaters. *Applied Energy* 84: 425-441.

[18] Yasin V. and H.F. Oztop, 2008. A comparative numerical study on natural convection in inclined wavy and flat plate solar collectors. *Building and Environment* 43: 1535-44.

[19] Kabeel A.E., Khalil A., Shalaby S.M. and Zayed M.E., 2016. Experimental investigation of thermal performance of flat and v-corrugated plate solar air heaters with and without PCM as thermal energy storage. *Energy Conversion and Management* 113: 264-272.

[20] Klein S.A., 1975. Calculation of flat plate loss coefficients. *Solar Energy* 17: 79-80.

[21] McAdams W.H., 1954. *Heat Transmission*. New York: McGraw-Hill.

[22] Hottel H.C. and B.B. Woertz. 1942. Performance of flat plate solar heat collectors. *Trans ASME* 64: 91-104.

[23] Heaton H.S., Reynolds W. and Kays W.M., 1964. Heat transfer in annular passages. Simultaneous development of velocity and temperature fields in laminar flow. *International Journal of Heat Mass Transfer* 7: 763-81.

[24] Kays W.M., 1980. *Convective Heat and Mass Transfer*. New York: McGraw Hill.

[25] Karim M.A., Perez E. and Amin Z.M., 2014. Mathematical modelling of counter flow v-grove solar air collector. *Renewable Energy* 67: 192-201.

[26] Hollands K.G.T. and E.C. Shewen. 1981. Optimization of flow passage geometry for air heating plate type solar collectors. *ASME J Solar Energy Eng* 103: 323-30.

[27] Ahmad A., Saini J.S. and Varma H.K., 1996. Thermohydraulic performance of packed bed solar air heaters. *Energy Conversion* 37: 205-214.

[28] Bahrehmand D., Ameri M. And Gholampour M., 2015. Energy and exergy analysis of different solar

air collector systems with forced convection. *Renewable Energy* 83: 1119-1130.

[29] Wong H.Y., 1977. *Handbook of essential formula and data on heat transfer for engineers*. London: Longman.

[30] Choudhury C., Andersen S.L. and Pekstad J., 1988. A solar air heater for low temperature applications. *Solar Energy* 40:77.

[31] Tan H.M. and W.W.S. Charters. 1969. Effect of thermal entrance region on turbulent forced convective heat transfer for an asymmetrically heated rectangular duct with uniform heat flux. *Solar Energy* 12: 513.

[32] Douglas J.F., Gasiorek J.M. and Swaffield J.A., 1992. *Fluid mechanics*. 2nd ed. England: Longman Singapore Publishers.

[33] Hegazy A.A., 2000. Thermohydraulic performance of air heating solar collectors with variable width, flat absorber plates. *Energy Conversion Management* 41:1361-78.

[34] Griggs E.I. and F.K. Sharifabad. 1992. Flow characteristics in rectangular ducts. *ASHRAE Trans* 98(1): 116-27.

[35] Akkawi M.A. and Z. Jaber. 2005. GIS: an integrated tool for power system planning based on spatial customer information. In the *Proceeding I of the 3rd International Conference on Education and Information Systems, Technologies and Applications (EISTA*, Orlando, Florida, USA. 14-17 July: 103-108.

APPENDIX A

$$J_1 = \frac{U_T + U_B + h_{c,ap-f2}}{U_T + U_B + h_{c,ap-f1} + h_{c,ap-f2}} \quad (1)$$

$$J_2 = \frac{h_{c,ap-f2}}{U_T + U_B + h_{c,ap-f1} + h_{c,ap-f2}} \quad (2)$$

$$J_3 = \frac{I\alpha_{ap}\tau_{gc}^2}{U_T + U_B + h_{c,ap-f1} + h_{c,ap-f2}} \quad (3)$$

$$J_4 = \frac{1}{h_{r,ap-gc1} + h_{c,f1-gc1} + U_{gc1-a}} \quad (4)$$

$$J_5 = \frac{U_T + U_B + h_{c,ap-f1}}{U_T + U_B + h_{c,ap-f1} + h_{c,ap-f2}} \quad (5)$$

$$J_6 = \frac{h_{c,ap-f1}}{U_T + U_B + h_{c,ap-f1} + h_{c,ap-f2}} \quad (6)$$

$$J_7 = \frac{1}{h_{r,ap-bp} + h_{c,f2-bp} + U_{bp-a}} \quad (7)$$

$$M_1 = -J_1 h_{c,ap-f1} - J_4 h_{c,f1-gc1} U_{gc1-a} - J_1 J_4 h_{c,f1-gc1} h_{r,ap-gc1} \quad (8)$$

$$M_2 = J_2 h_{c,ap-f1} + J_2 J_4 h_{c,f1-gc1} h_{r,ap-gc1} \quad (9)$$

$$M_3 = J_3 h_{c,ap-f1} + J_3 J_4 h_{c,f1-gc1} h_{r,ap-gc1} \quad (10)$$

$$M_4 = J_6 h_{c,ap-f2} + J_6 J_7 h_{c,f2-bp} h_{r,ap-bp} \quad (11)$$

$$M_5 = -J_5 h_{c,ap-f2} - J_7 h_{c,f2-bp} U_{bp-a} - J_5 J_7 h_{c,f2-bp} h_{r,ap-bp} \quad (12)$$

$$M_6 = J_3 h_{c,ap-f2} + J_3 J_7 h_{c,f2-bp} h_{r,ap-bp} \quad (13)$$

$$Y_1 = \frac{1}{2}\left[\left(\frac{M_1}{\varphi} + \frac{M_5}{(1-\varphi)}\right) + \sqrt{\left(\frac{M_1}{\varphi} - \frac{M_5}{(1-\varphi)}\right)^2 + \frac{4M_2M_4}{\varphi(1-\varphi)}}\right] \quad (14)$$

$$Y_2 = \frac{1}{2}\left[\left(\frac{M_1}{\varphi} + \frac{M_5}{(1-\varphi)}\right) - \sqrt{\left(\frac{M_1}{\varphi} - \frac{M_5}{(1-\varphi)}\right)^2 + \frac{4M_2M_4}{\varphi(1-\varphi)}}\right] \quad (15)$$

$$C_1 = -\left[\left(\frac{\frac{M_4}{1-\varphi} + \frac{M_5}{1-\varphi} - Y_2}{Y_2 - Y_1}\right)(T_{f,in} - T_a) + \left(\frac{Y_2}{Y_2 - Y_1}\right)\left(\frac{M_3M_4 - M_1M_6}{M_1M_5 - M_2M_4}\right) + \frac{M6}{1-\varphi Y2 - Y1}\right] \quad (16)$$

$$C_2 = \left(\frac{\frac{M_4}{1-\varphi} + \frac{M_5}{1-\varphi} - Y_1}{Y_2 - Y_1}\right)(T_{f,in} - T_a) + \left(\frac{Y_1}{Y_2 - Y_1}\right)\left(\frac{M_3M_4 - M_1M_6}{M_1M_5 - M_2M_4}\right) + \frac{\frac{M_6}{1-\varphi}}{Y_2 - Y_1} \quad (17)$$